J. Ocean Univ. China (Oceanic and Coastal Sea Research)
DOI 10.1007/s11802-015-2421-7
ISSN 1672-5182, 2015 14 (2): 191-198
http://www.ouc.edu.cn/xbywb/
E-mail:xbywb@ouc.edu.cn

Impacts of the Two Types of El Niño on Pacific Tropical Cyclone Activity

XU Shibin[1), 2)], and HUANG Fei[1), 3), *]

1) *Physical Oceanography Laboratory & Key Laboratory of Ocean-Atmosphere Interaction and Climate in Universities of Shandong*, *Ocean University of China*, *Qingdao* 266100, *P. R. China*
2) *International Pacific Research Center*, *School of Ocean and Earth Science and Technology*, *University of Hawaii at Manoa*, *Honolulu*, *HI* 96822, *USA*
3) *Ningbo Collabrative Innovation Center of Nonlinear Harzard System of Ocean and Atmosphere*, *Ningbo University*, *Ningbo* 315211, *P. R. China*

(Received June 18, 2013; revised December 16, 2013; accepted December 29, 2014)

Abstract It is well known that Tropical cyclone (TC) activities over the Pacific are affected by El Niño events. In most studies El Niño phenomena have been separated into east Pacific warming (EPW) and central Pacific warming (CPW) based on the location of maximum SST anomaly. Since these two kinds of El Niño have different impacts on Pacific tropical cyclone activities, this study investigates different features of TC activities and the genesis potential index (GPI) during EPW years and CPW years. Four contributing factors, *i.e.*, the low-level absolute vorticity, the relative humidity, the potential intensity and the vertical wind shear, are examined to determine which factors are most important in causing the anomalous TC activities. Our results show that during EPW years in July–August (JA^0), TC activities are more frequent with stronger intensity over the Western North Pacific (WNP) and Eastern North Pacific (ENP). The maximum anomaly center of TC activities then drifts eastward significantly in September–October (SO^0). However, centers of anomalous TC activity barely change from JA^0 to SO^0 during CPW years. In January–February–March (JFM^1) of the decaying years of warming events, TC frequency and intensity both have positive anomaly over the South Pacific. The anomalies in EPW years have larger amplitude and wider spatial distribution than those in CPW years. These anomalous activities of TC are associated with GPI anomaly and the key factors affecting GPI anomaly for each ocean basin are quite different.

Key words tropical cyclone; eastern pacific warming; central pacific warming; GPI

1 Introduction

There are many studies about the influence of El Niño and Southern Oscillation (ENSO) on tropical cyclone (TC) activities over the Pacific. One general consensus is that the location of TC formation would shift eastward in strong El Niño years. In the summer and autumn when El Niño TC activities are intensified over the south eastern WNP, TCs would cover larger areas with longer duration over the warm sea surface before landing. As a result, the average intensity of TC would become stronger in El Niño years (Chan, 2000; Wang and Chan, 2002; Chen *et al.*, 2006). In La Niña years the situation is reversed. Vertical wind shear and low-level vorticity changes caused by anomalous circulation play more important roles than local SST in TC activity (Camargo and Sobel, 2005; Chen and Huang, 2006), indicating the importance of dynamic process in TC activities. Significant impact of El Niño on eastern North Pacific TC activities is clearly illustrated by westward drifting of TC genesis location and maximum intensity location during El Niño years. The number of intense TCs tends to increase in El Niño years (Irwin and Davis, 1999; Camargo *et al.*, 2008; Clark and Chu, 2002). In the south Pacific, ENSO is the main factor responsible for the inter-annual variation of TC activities and there are more TCs over the south Pacific during El Niño years. Changes in large scale circulation patterns associated with El Niño appear to be the key factors affecting TC activeties. Previous studies (Evans and Allan, 2006; Kuleshov *et al.*, 2009; Ramsay *et al.*, 2008; Liu and Chan, 2010) have shown that the low level vorticity would be enhanced over the Western South Pacific as a response to the SST warming in the eastern equatorial Pacific, thus the TC activities tend to be enhanced in this situation.

Recent studies showed that the location of maximum SST anomaly tended to shift to the central Pacific during some El Niño events in the past two decades (Kao and Yu, 2009). Hence El Niño events have been separated into two types according to the location of maximum SST anomaly: the Central Pacific Warming (CPW) and the

* Corresponding author. Tel: 0086-532-66781305
E-mail: huangf@ouc.edu.cn

Eastern Pacific Warming (EPW). In some studies the EPW was named as the dateline El Niño (Larkin and Harrison, 2005), the El Niño Modoki (Ashok *et al.*, 2007) or the warm pool El Niño (Kug *et al.*, 2009). Both of the two types of El Niño have influence on large-scale circulation of the Pacific region (Yeh *et al.*, 2009) while responses of the large-scale circulation to each warming pattern are different. Some studies have shown that the two types of the tropical Pacific warming would induce different TC activity anomalies, for instance the genesis number and tracks (Kim *et al.*, 2009, 2011a; Chen and Tam, 2010; Wang *et al.*, 2014; Wang and Wang, 2013a). Furthermore, different type of El Niño may have variable influence on the TC activities in the next summer through the different response of Indian Ocean to types of El Niño (Du *et al.*, 2011; Wang and Wang, 2013b). However, more details of TC activity anomaly during EPW and CPW are not yet known and need to be addressed over the entire Pacific.

In this study, the variability of TC activity over the Pacific during EPW years and CPW years was investigated in terms of TC frequency (represented by storm days) and intensity (represented by maximum wind speed). The genesis potential index (GPI) is used to explain the TC activity anomaly. Four contributing factors, *i.e.*, the low-level absolute vorticity, the relative humidity, the potential intensity and the vertical wind shear, are examined to determine which factor or factors are the most important in causing the anomalous TC activities.

This paper is organized as follows. Data and methodology used in this study are introduced in Section 2. Characters of TC activity anomaly during EPW and CPW years are described in Section 3. The GPI anomalies during the two types of warming events are analyzed in Section 4. Finally, conclusions of this study are presented in Section 5.

2 Data and Methodology

This study covers the period of 1971 to 2010. TC datasets over the Pacific archived in the International Best Track Archive for Climate Stewardship (IBTrACS) are obtained to investigate features of TC activities in the Pacific. Since the main tropical cyclone season of the North Pacific is from July to October (JASO) and its counterpart of the south Pacific is from January to March (JFM), the present study focuses on the summer and fall during warming events developing years in the North Pacific, and the spring during warming events decaying years in the south Pacific. For convenience, we use JA^0 and SO^0 to represent July-August and September-October of El Niño developing years while JFM^1 to represent January-February-March of El Niño decaying years. TC frequency and intensity are calculated based on the 6-hour interval data archived in IBTrACS. Only those TCs with maximum surface wind greater than 34 knots are considered.

The multi-level daily atmospheric data include wind, air temperature, relative humidity, surface temperature and pressures with resolution of 2.5°×2.5° for the period 1971 to 2010 derived from NCEP/NCAR Reanalysis data (Kalnay *et al.*, 1996).

Since there are different definitions of CPW years and EPW years, the classification of warming events are different for some years. For instance, the warming events in 1977 (Kug *et al.*, 2009), 1990 (Ashok *et al.*, 2007) and 1991 (Kim *et al.*, 2011b) are classified into different kinds based on variable definitions. In the fallowing sections only the EPW years and CPW years that are in agreement by various definitions are considered (Ashok *et al.*, 2007; Kao and Yu, 2009; Kug *et al.*, 2009; Kim *et al.*, 2011b; Ratnam *et al.*, 2012). As a result, four typical CPW years (1994, 2002, 2004 and 2009) and four typical EPW years (1972, 1976, 1982 and 1997) were chosen for investigation in this study.

3 TC Activity Anomaly During the Pacific Warming Events

Wang *et al.* (2010) have shown that storm-days in the Pacific can be affected by ENSO events. Since large-scale circulations of the ocean and the atmosphere have different responses to EPW and CPW events respectively, TC activities over the Pacific are expected to have different characteristics during EPW and CPW years. TC frequency and intensity are used to investigate the TC activity features over the Pacific during these two types of warming events.

3.1 TC Frequency

Fig.1 shows the composites of mean storm-days anomalies in JA^0, SO^0 and JFM^1 of EPW years and CPW years. Storm-days is defined as the number of tropical cyclones occurrence in each grid box based on the 6-hour record. Storm-days anomaly is calculated by removing the 40-year climatology average for the period 1971 to 2010.

In JA^0 of EPW years, there were more TC activities over most areas of the western north Pacific (WNP) (Fig.1a). At the same time, TC activity was suppressed near the Mexico coast and enhanced over other parts of the eastern north Pacific (ENP). The TC activities also increased over the WNP and the ENP during JA^0 of CPW years (Fig.1b). There was significantly positive storm-days during the CPW events appearing in the central Pacific but this cannot be found during EPW years. The impacts of EPW events and CPW events on the ENP and WNP TC activity were similar in JA^0 although the SST anomalies appeared in different locations. CPW events can also increase the TC activity over the central Pacific.

In SO^0 of EPW years, TC activities were significantly decreased over the west part of the WNP but increased over the east part of the WNP (Fig.1c). This pattern means that location of positive anomaly of storm-days shifted eastward from JA^0 to SO^0. The anomalous center in ENP also shifted eastward. In contrast, the positive anomaly of storm-days was still dominant over the broad

area of WNP and ENP during CPW years (Fig.1d).

In JFM^1 of EPW years, areas of positive anomaly of storm-days were located over the South Pacific and the main body of storm-days anomaly was located on the west side of the dateline (Fig.1e). However, in JFM^1 of CPW year, the main body of positive anomaly of storm days was located on the east side of the dateline (Fig.1f).

3.2 TC Intensity

TC intensity also can be influenced by ENSO. Many studies show that there would have more intense TCs in El Niño years over WNP (Camargo and Sobel, 2005; Huang and Xu, 2010; Zhao *et al.*, 2011). In this paper, wind speed is used to examine the TC intensity during the two types of El Niño. The averaged wind speed is defined as the average of maximum wind of TC occurring in each grid box based on the 6-hour record. TC intensity anomaly is obtained by removing the 40-year mean.

Fig.2 shows the composites of the averaged wind speed anomalies in JA^0, SO^0 and JFM^1 of EPW and CPW years. In JA^0 of EPW years TC intensity was enhanced over most areas of both the WNP and the ENP except over the South China Sea and the Mexico coast (Fig.2a). The TC intensity had barely changes over the South China Sea and had a decrease near the Mexico coast. Similarly, TC intensity had positive anomaly over the broad area of the North Pacific but it was negative of the eastern and western edges of the north Pacific in JA^0 of CPW years (Fig.2b).

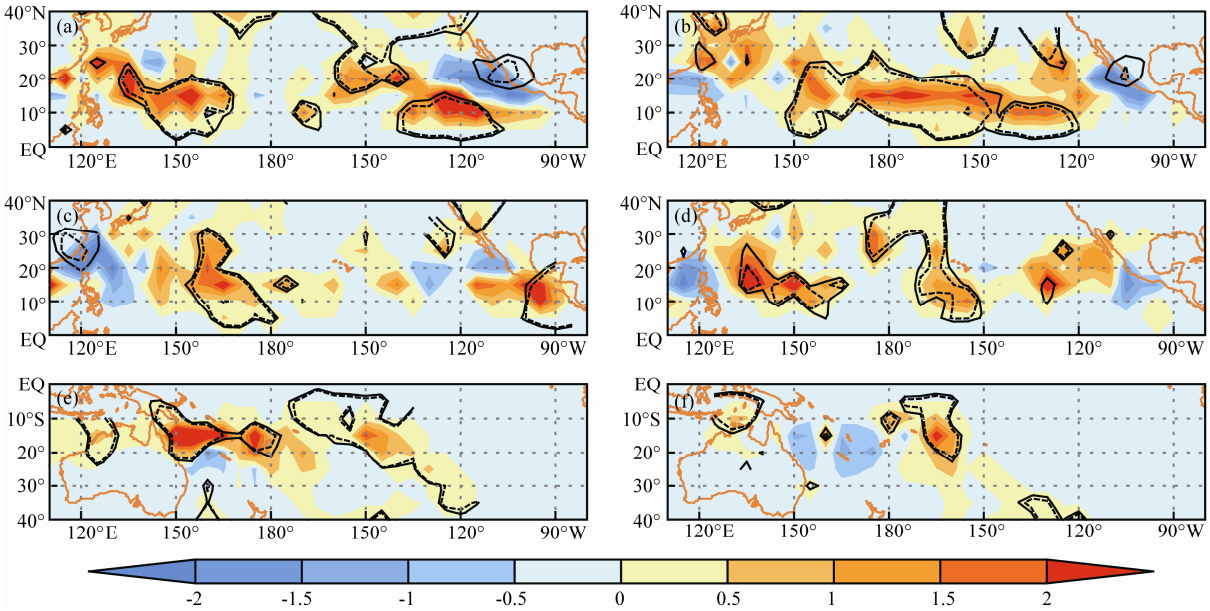

Fig.1 Storm-days anomalies in JA^0 (a, b), SO^0 (c, d) and JFM^1 (e, f) during EPW years (left) and CPW years (right). The solid line shows the 90% confidence level and the dash line shows the 95% confidence level by *t*-test.

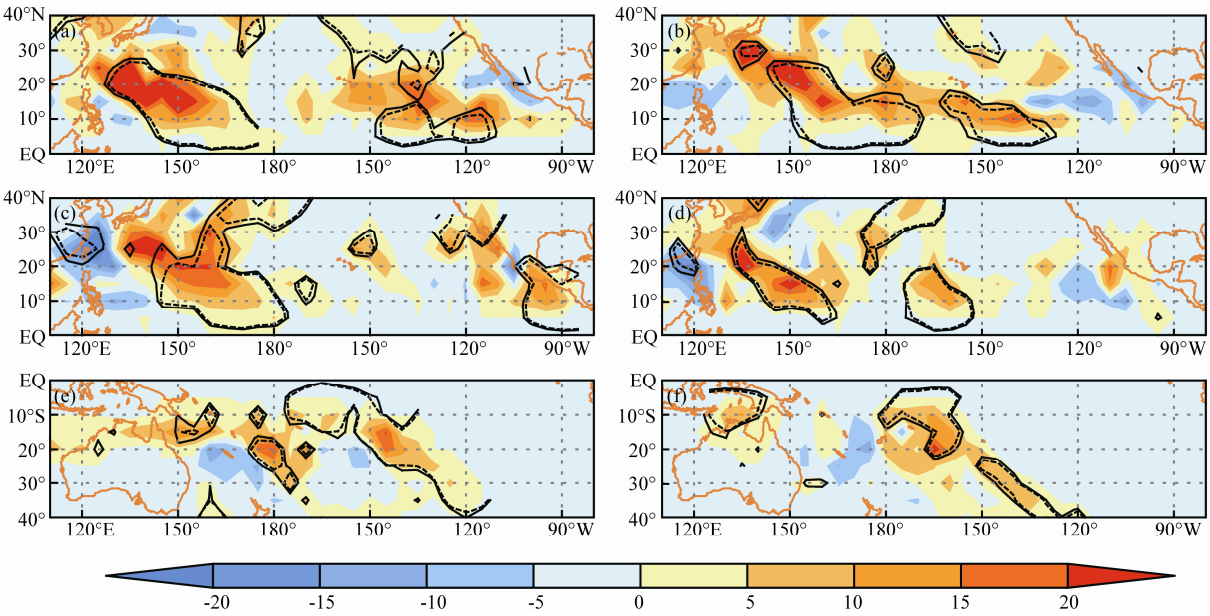

Fig.2 TC intensity anomaly JA^0 (a, b), SO^0 (c, d) and JFM^1 (e, f) during EPW years (left) and CPW years (right). The solid line shows the 90% confidence level and the dash line shows the 95% confidence level by *t*-test.

In SO^0 of EPW years, TC intensity anomaly shifted more eastward than that in JA^0. This means TC intensity decreased over the Philippians Sea and the East China Sea. Changes in TC intensity were not significant over the NEP during this time (Fig.2c). In contrast, the location of TC intensity anomaly over the WNP in SO^0 of CPW years was close to that in JA^0, but the increasing of TC intensity over ENP was not as significant as that in JA^0 (Fig.2d).

TC intensity over the SP had different response to warm events in EPW years and CPW years in the fallowing JFM[1]. It had positive anomaly over the SP in EPW year and CPW years while the spatial distribution and the amplitude were larger in EPW years than those in CPW years (Figs.2e, 2f).

4 GPI Anomaly During the Two Types of Pacific Warming

Emanuel and Nolan (2004) defined a genesis potential index (GPI) to examine the climate factors for TC activity. The GPI is composed of low-level absolute vorticity, relative humidity, potential intensity and vertical wind shear. The potential intensity depends on SST, air temperature and sea level pressure (Bister and Emanuel, 2002). The GPI is defined as

$$GPI = |10^5 \eta|^{3/2} \left(\frac{H}{50}\right)^3 \left(\frac{PI}{70}\right)^3 (1+0.1V_{\text{shear}})^{-2},$$

where η is the absolute vorticity at 850 hPa, H is the relative humidity at 700 hPa, PI is the potential intensity of TC and V_{shear} is the vertical wind shear between 850 hPa and 200 hPa. To examine the influence of environmental factors on tropical cyclone activity, the GPI is first calculated by daily data, and then averaged to obtain the monthly mean of GPI. The anomaly of GPI is obtained by removing the 40-year climatology for the period 1971 to 2010 from the original GPI.

To compare the importance of the four variables which are used in the GPI calculation, we calculated GPI* using the climatology of three of the variables and original value of the fourth variable. This process was repeated for all variables. Although the anomaly of GPI is not the sum of the four GPI*, the contribution of each variable to the GPI can be described.

Fig.3 shows the composite of GPI anomaly and GPI* anomalies for each variable in JA^0 of EPW years and CPW years. In EPW year, GPI over the WNP showed positive anomaly on the southeast part and negative anomaly on the northwest part (Fig.3a). Although the positive GPI anomaly was not adjacent to the Asia continent, most TCs moved westward or northwestward after

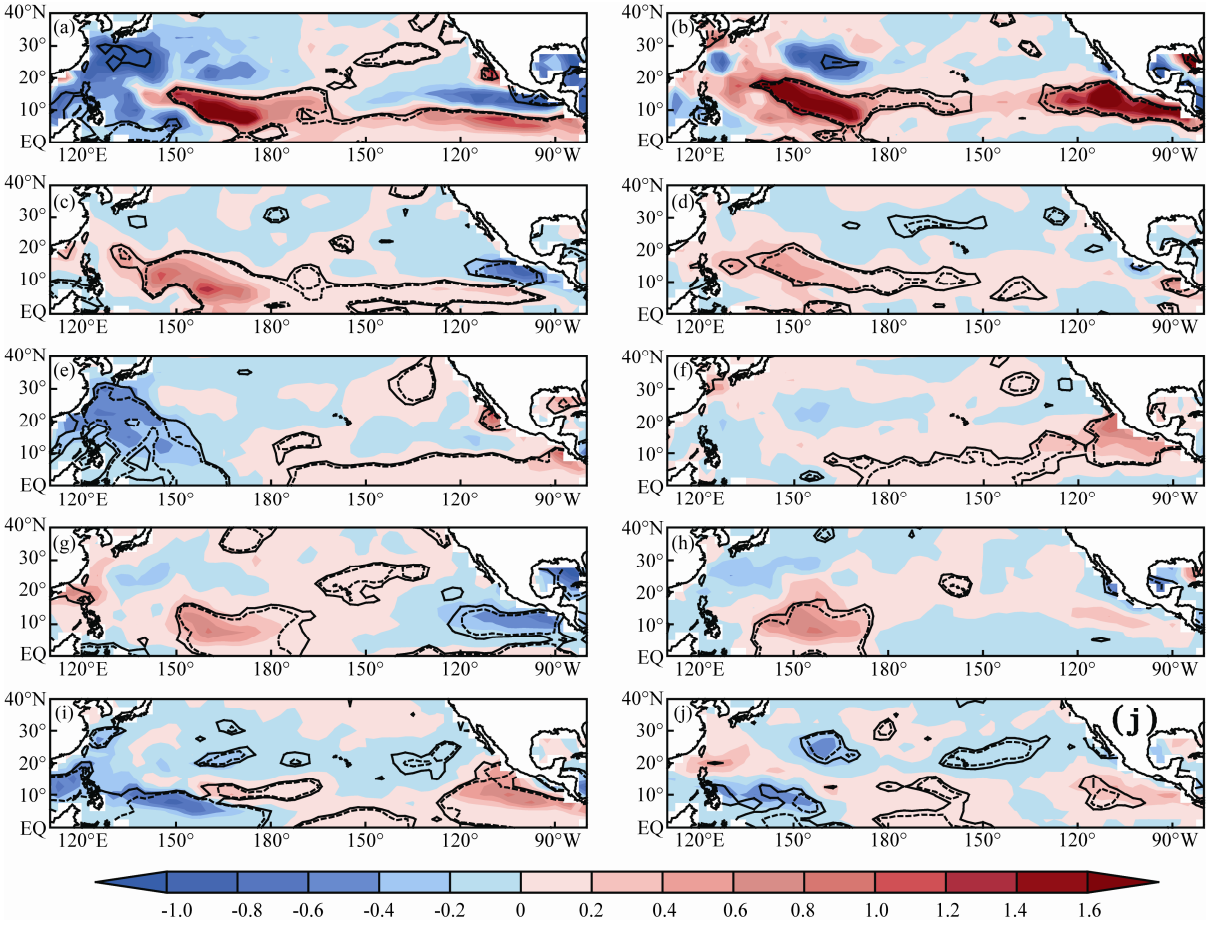

Fig.3 GPI anomaly in JA^0 of EPW years (a) and CPW years (b), and GPI* for (c, d) the low level vorticity, (e, f) PI, (g, h) the relative humidity and (i, j) the vertical wind shear in JA^0 of EPW years (left) and CPW years (right). The solid line shows the 90% confidence level and the dash line shows the 95% confidence level by *t*-test.

their genesis. As a result, the positive TC activity extended to the Asian coast (Fig.1a). GPI* for different factors show very different patterns. The increase of GPI was mainly owing to the positive relative humidity anomaly (Fig.3g) and low-level vorticity (Fig.3c) which were caused by a deeper summer monsoon trough. The decrease of GPI over the East China Sea was mainly due to the negative PI anomaly (Fig.3c), while the negative GPI over the southern part of Philippine Sea was mainly due to the vertical wind shear anomaly (Fig.3i). In ENP, the positive GPI anomaly was located to the south of 10˚N and negative GPI anomaly was located to the north of 10˚N (Fig.3a). Thus the TC activity anomaly showed a south-north dipole pattern over the ENP (Fig.1a). Decreased vertical wind shear was the main contributor of the positive GPI anomaly to the south of 10˚N (Fig.3i), while the negative GPI to the north of 10˚N anomaly was mainly caused by the decreased low-level vorticity (Fig.3c) and negative 700 hPa relative humidity (Fig.3g). In contrast, the GPI positive anomaly dominated WNP and ENP in JA^0 of CPW years (Fig.3b). The positive GPI anomaly extended a little northward than that in EPW years, thus the positive TC activities extended northward to a bit higher latitude than its counterpart in EPW years (Fig.1b). The increase of GPI in WNP was mainly owing to the increased relative humidity (Fig.3h) and positive low-level vorticity anomaly (Fig.3j), while the PI and vertical wind shear had no significant changes over WNP. The increase of GPI in ENP was mainly owing to lager PI (Fig.3f) and minor vertical wind shear (Fig.3j). The low level vorticity and relative humidity had barely changes over ENP.

The composite of GPI anomaly and GPI* anomaly for each variable in SO^0 of EPW years and CPW years are shown in Fig.4. The positive GPI anomaly over the WNP shifted to central Pacific in SO^0 during EPW years, hence the negative GPI anomaly dominated most areas of the WNP (Fig.4a). This GPI anomaly dipole pattern induced the decreased TC storm-days over the west part of the WNP and increased TC storm-days over the east part of the WNP (Fig.1c). The main contributing factors to the negative GPI anomaly over the South China Sea and Philippine Sea were 700 hPa relative humidity (Fig.4g) and low-level vorticity (Fig.4c). The key factors that caused the negative GPI anomaly to the east of the Philippine Sea are the 700 hPa relative humidity (Fig.4g) and the vertical wind shear (Fig.4i). The negative low-level

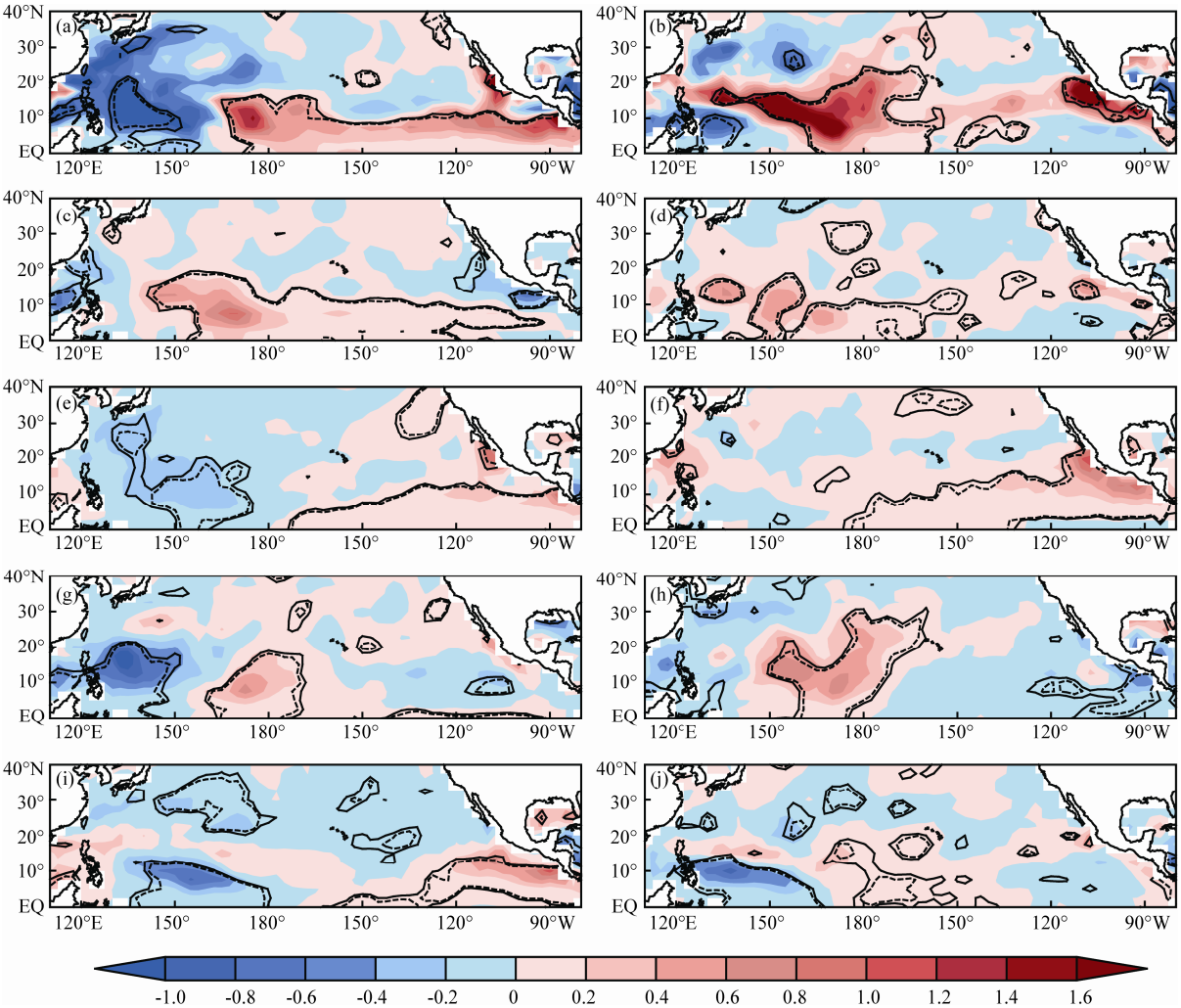

Fig.4 GPI anomaly in SO^0 of EPW years (a) and CPW years (b), and GPI* for (c, d) the low level vorticity, (e, f) PI, (g, h) the relative humidity and (i, j) the vertical wind shear in SO^0 of EPW years (left) and CPW years (right). The solid line shows the 90% confidence level and the dash line shows the 95% confidence level by *t*-test.

vorticity was caused by the Philippine Sea anticyclone anomaly (Wang *et al.*, 2000). The anomalous northern wind on the east part of the anticyclone resulted in negative humidity anomaly on 700 hPa. The positive GPI anomaly over the ENP was mainly due to the vertical wind shear (Fig.4i) and PI (Fig.4e). The positive GPI anomaly was still dominant over the main area of the WNP despite the fact that there were negative GPI anomaly near Japan and southern part of the Philippine Sea in SO^0 of CPW years (Fig.4b). As a result, positive TC activities still dominanted the WNP during SO^0 of CPW years (Fig.1d). The positive GPI anomaly was mainly due to the low-level vorticity (Fig.4d) and the relative humidity on 700 hPa (Fig.4h). The negative GPI anomalies near Japan and over the southern Philippine Sea were mainly owing to the relative humidity (Fig.4h) and vertical wind shear (Fig.4i) respectively. The positive GPI anomaly over the ENP was mainly owing to PI (Fig.4f) and the low-level vorticity (Fig.4d).

The composite of GPI anomaly and GPI* anomaly for each variable over SP in JFM^1 during EPW events and CPW events are shown in Fig.5. In JFM^1 of EPW years, a south-north dipole pattern of GPI anomaly appeared in TC genesis region, *i.e.*, it was positive on the southern part and negative on the northern part (Fig.5a). This pattern induced more TC activities over the north part of SP during JFM^1 of EPW years (Fig.1e). The low-level vorticity (Fig.5c), the 700 hPa relative humidity (Fig.5g) and the vertical wind shear (Fig.5i) were major contributors to positive GPI anomaly, while the negative GPI anomaly was mainly due to PI (Fig.5e) and the vertical wind shear (Fig.5i) in this area. In JFM^1 of CPW years, the GPI anomaly also showed a south-north dipole pattern (Fig.5b). The location of extremely anomalous centers shifted westward and the amplitudes were smaller than that of EPW years, hence the TC activity anomaly was not as obvious as that in EPW years (Fig.1f). The positive GPI anomaly was mainly owing to the low-level vorticity (Fig.5d), the 700 hPa relative humidity (Fig.5h) and vertical wind shear (Fig.5j). The negative GPI anomaly was mainly owing to the vertical wind shear in the southern part of TC genesis region (Fig.5j). Low level vorticity, PI and the relative humidity at 700 hPa also contributed to this negative anomaly.

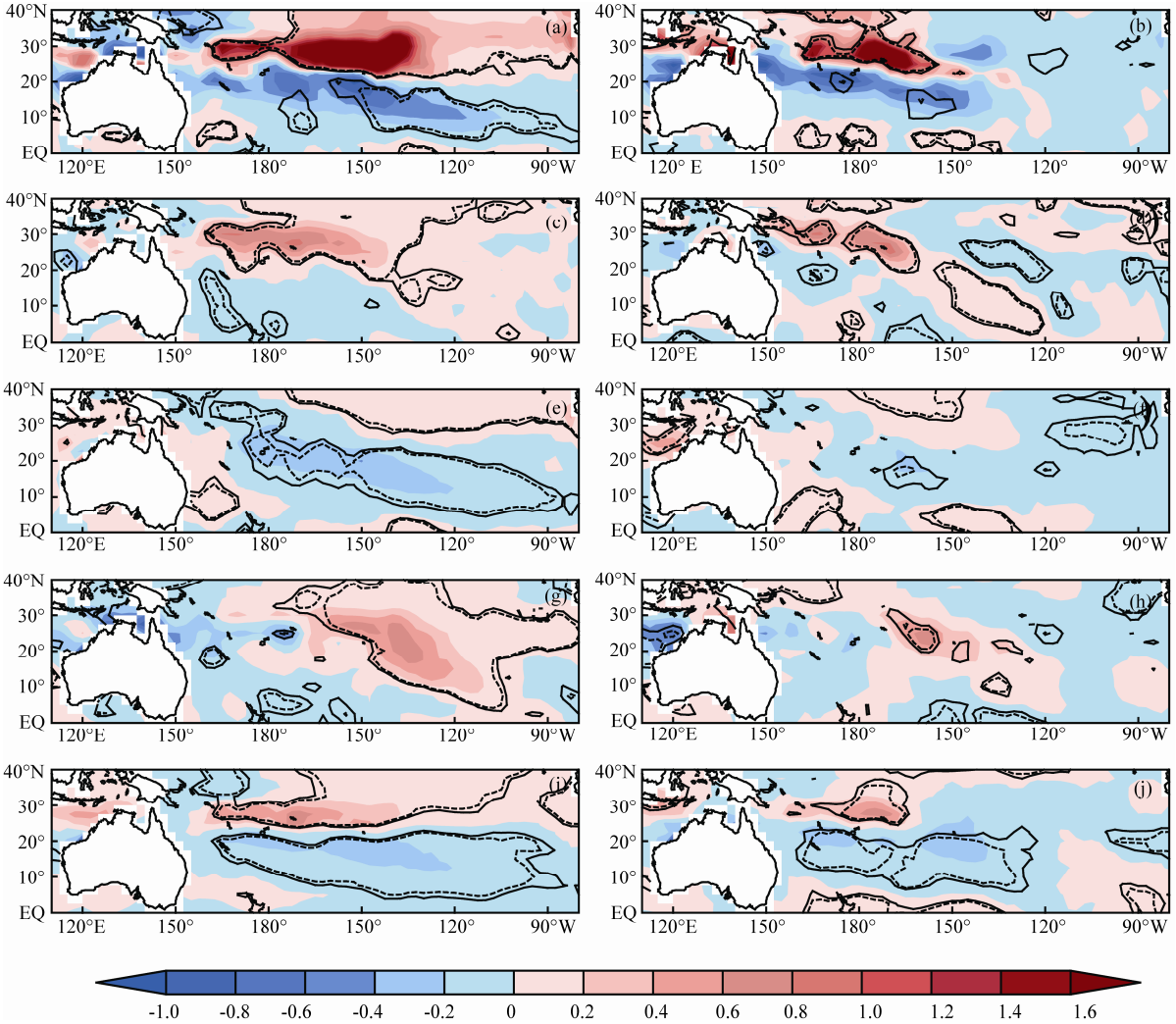

Fig.5 GPI anomaly in JFM^1 of EPW years (a) and CPW years (b), and GPI* for (c, d) the low level vorticity, (e, f) PI, (g, h) the relative humidity and (i, j) the vertical wind shear in JFM^1 of EPW years (left) and CPW years (right). The solid line shows the 90% confidence level and the dash line shows the 95% confidence level by *t*-test.

5 Summary and Discussion

In this study, the influence of two types of El Niño on the Pacific tropical cyclone activity has been investigated by diagnosing the TC frequency and intensity. To compare the different characters during EPW and CPW events, TC frequency and intensity are composited on 4 typical EPW years and 4 typical CPW years.

The result shows that in JA^0 of EPW years, there were more and stronger TCs over WNP and ENP. In SO^0, TC activity was suppressed over the western part and enhanced over the eastern part of WNP. In ENP the maximum anomaly centers also significantly drifted eastward in SO^0. In the fallowing JFM^1, there were more TCs over the South Pacific and the maximum center was located on the west side of date line.

In JA^0 of CPW years, TC activity was increased over the entire WNP and ENP except over the South China Sea and the Mexico coast area. This pattern persisted to SO^0. In the fallowing JFM^1, TC activity increased over SP with smaller amplitude and a narrower spatial distribution than that in EPW events.

TC activity anomalies were induced by the thermal-dynamic changes of large scale circulations in both EPW and CPW years. To investigate the key factors affecting TC activities, GPI and GPI* for each parameter were investigated. During both of CPW and EPW events, the positive GPI anomaly over WNP was mainly caused by the positive low level absolute vorticity and 700 hPa relative humidity anomalies. The negative GPI anomaly near the Asian coast was mainly due to smaller PI and larger wind shear in JA^0 of EPW years. The 700 hPa relative humidity and the vertical wind shear were the two key factors that caused negative GPI anomaly in SO^0 of EPW years. In contrast, the anomalous GPI over ENP was mainly owing to the vertical wind shear and the MPI. The key factors affecting positive GPI over SP in JFM^1 were the low-level vorticity, the 700 hPa relative humidity and the vertical wind shear while the PI and the vertical wind shear played very important rules in the negative GPI anomaly.

Acknowledgements

We would like to thank Prof. Bin Wang from University of Hawaii for his constructive suggestions and Dr. Ming Chen at NCAR for her English revision. This work was supported by the National Basic Research Program of China (973 Program: 2012CB955604), NSFC-Shangdong Joint Fund for Marine Science Research Centers (U14064 01), and the CMA Program (GYHY200906008).

References

Ashok, K., Behera, S. K., Rao, S. A., Weng, H., and Yamagata, T., 2007. El Niño Modoki and its possible teleconnection. *Journal of Geophysical Research*, **112**, C11007, DOI: 10.1029/2006JC003798.

Bister, M., and Emanuel, K. A., 2002. Low frequency variability of tropical cyclone potential intensity 1. Interannual to interdecadal variability. *Journal of Geophysical Research*, **107**: 4801, DOI: 10.1029/2001JD000776.

Camargo, S. J., and Sobel, A. H., 2005. Western North Pacific tropical cyclone intensity and ENSO. *Journal of Climate*, **18**: 2996-3006, DOI: 10.1175/JCLI3457.1.

Camargo, S. J., Robertson, A. W., Barnston, A. G., and Ghil, M., 2008. Clustering of eastern North Pacific tropical cyclone tracks: ENSO and MJO effects. *Geochemistry, Geophysics and Geosystems*, **9**, Q06V05, DOI: 10.1029/2007GC001861.

Chan, C. L., 2000. Tropical cyclone activity over the Western North Pacific associated with El Niño and La Niña events. *Journal of Climate*, **13**: 2960-2972, DOI: 10.1175/1520-0442(2000)013<2960:TCAOTW>2.0.CO;2.

Chen, G., and Tam, C. Y., 2010. Different impacts of two kinds of Pacific Ocean warming on tropical cyclone frequency over the western North Pacific. *Geophysical Research Letters*, **37**, L01803, DOI: 10.1029/2009GL041708.

Chen, G., and Huang, R., 2006. The effect of warm pool thermal states on tropical cyclone in West Northwest Pacific. *Journal of Tropical Meteorology*, **22** (6): 527-532.

Chen, T. C., Wang, S. Y., and Yen, M. C., 2006. Interannual variation of the tropical cyclone activity over the Western North Pacific. *Journal of Climate*, **19**: 5709-5720, DOI: 10.1175/JCLI3934.1.

Clark, J. D., and Chu, P. S., 2002. Interannual variation of tropical cyclone activity over the central North Pacific. *Journal of the Meteorological Society of Japan*, **80** (3): 403-418.

Du, Y., Yang, L., and Xie, S.-P., 2011. Tropical Indian Ocean influence on Northwest Pacific tropical cyclones in summer following strong El Niño. *Journal of Climate*, **24** (1): 315-322.

Emanuel, K. A., and Nolan, D. S., 2004. Tropical cyclones activity and the global climate system. Presented at 26th Conference on Hurricanes and Tropical Meteorology, American Meteorological Society, Miami, Fla, 240-241.

Evans, J. L., and Allan, R. J., 2006. El Niño Southern Oscillation modification to the structure of the monsoon and tropical cyclone activity in the Australasian region. *International Journal of Climatology*, **12** (6): 611-623, DOI: 10.1002/joc.3370120607.

Huang, F., and Xu, S., 2010. Super typhoon activity over the western North Pacific and its relationship with ENSO. *Journal of Ocean University of China*, **9** (2): 123-128, DOI: 10.1007/s11802-010-0123-8.

Irwin, R. P., and Davis, R. E., 1999. The relationship between the Southern Oscillation Index and tropical cyclone tracks in the eastern North Pacific. *Geophysical Research Letters*, **26** (15): 2251-2254, DOI: 10.1029/1999GL900533.

Kao, H.-Y., and Yu, J.-Y., 2009. Contrasting Eastern-Pacific and Central-Pacific types of ENSO. *Journal of Climate*, **22**: 615-632, DOI: 10.1175/2008JCLI2309.1.

Kalnay, E., Kanamitsu, M., Kistler, R., Collins, W., Deaven, D., Gandin, L., Iredell, M., Saha, S., White, G., Woollen, J., Zhu, Y., Leetmaa, A., Reynolds, R., Chelliah, M., Ebisuzaki, W., Higgins, W., Janowiak, J., Mo, K. C., Ropelewski, C., Wang, J., Jenne, R., and Joseph, D., 1996. The NCEP/NCAR 40-year reanalysis project. *Bulletin of the American Meteorological Society*, **77**: 437-470, DOI: 10.1175/1520-0477(1996)077<0437:TNYRP>2.0.CO;2.

Kim, H.-M., Webster, P. J., and Curry, J. A., 2009. Impact of shifting patterns of Pacific Ocean warming on north Atlantic tropical cyclones. *Science*, **325**: 77-79, DOI: 10.1126/science.

1174062.

Kim, H. M., Webster, P. J., and Curry, J. A., 2011a. Modulation of North Pacific tropical cyclone activity by three phases of ENSO. *Journal of Climate*, **24**: 1839-1849, DOI: 10.1175/2010JCLI3939.1.

Kim, W., Yeh, S.-W., Kim, J.-H., Kug, J.-S., and Kwon, M., 2011b. The unique 2009–2010 El Niño event: A fast phase transition of warm pool El Niño to La Niña. *Geophysical Research Letters*, **38**, L15809, DOI: 10.1029/2011GL048521.

Kug, J.-S., Jin, F.-F., and An, S.-I., 2009. Two types of El Niño events: Cold tongue El Niño and warm pool El Niño. *Journal of Climate*, **22**: 1499-1515, DOI: 10.1175/2008JCLI2624.1.

Kuleshov, Y., Chane Ming, F., Qi, L., Chouaibou, I., Hoareau, C., and Roux, F., 2009. Tropical cyclone genesis in the Southern Hemisphere and its relationship with the ENSO. *Annales Geophysicae*, **27**: 2523-2538, DOI:10.5194/angeo-27-2523-2009.

Larkin, N. K., and Harrison, D. E., 2005. Global seasonal temperature and precipitation anomalies during El Niño autumn and winter. *Geophysical Research Letters*, **32**, L13705, DOI: 10.1029/2005GL022738.

Liu, K. S., and Chan, J. C. L., 2010. Interannual variation of southern hemisphere tropical cyclone activity and seasonal forecast of tropical cyclone number in the Australian region. *International Journal of Climatology*, **32** (2): 190-202, DOI: 10.1002/joc.2259.

Ramsay, H. A., Leslie, L. M., Lamb, P. J., Richman, M. B., and Leplastrier, M., 2008. Interannual variability of tropical cyclones in the Australian region: Role of large-scale environment. *Journal of Climate*, **21**: 1083-1103, DOI: 10.1175/2007JCLI1970.1.

Ratnam, J. V., Behera, S. K., Masumoto, Y., Takahashi, K., and Yamagata, T., 2012. Anomalous climatic conditions associated with the El Niño Modoki during boreal winter of 2009. *Climate Dynamics*, **39**: 227-238, DOI: 10.1007/s00382-011-1108-z.

Wang, B., Wu, R., and Fu, X., 2000. Pacific-East Asia teleconnection: How does ENSO affect East Asian climate? *Journal of Climate*, **13**: 1517-1536, DOI: 10.1175/1520-0442(2000)013<1517:PEATHD>2.0.CO;2.

Wang, B., and Chan, J. C. L., 2002. How strong ENSO affect tropical storm activity over the Western North Pacific. *Journal of Climate*, **15**: 1643-1658, DOI: 10.1175/1520-0442(2002)015<1643:HSEEAT>2.0.CO;2.

Wang, B., Yang, Y., Ding, Q., Murakami, H., and Huang, F., 2010. Climate control of the global tropical storm days (1965–2008). *Geophysical Research Letters*, **37**, L07704, DOI: 10.1029/2010GL042487.

Wang, C., and Wang, X., 2013a. Classifying El Niño Modoki I and II by different impacts on rainfall in southern China and typhoon tracks. *Journal of Climate*, **26**: 1322-1338, DOI: 10.1175/JCLI-D-12-00107.1.

Wang, X., Zhou, W., Li, C., and Wang, D., 2014. Comparison of the impact of two types of El Niño on tropical cyclone genesis over the South China Sea. *International Journal of Climatology*, **34** (8): 2651-2660, DOI: 10.1002/joc.3865.

Wang, X., and Wang, C., 2013b. Different impacts of various El Niño events on the Indian Ocean Dipole. *Climate Dynamics*, doi: 10.1007/s00382-013-1711-2.

Yeh, S.-W., Kug, J.-S., Dewitte, B., HoKwon, M., Kirtman, B. P., and Jin, F.-F., 2009. El Niño in a changing climate. *Nature*, **461**: 511-515, DOI: 10.1038/nature08316.

Zhao, H., Wu, L., and Zhou, W., 2011. Interannual changes of tropical cyclone intensity in the western North Pacific. *Journal of the Meteorology Society of Japan*, **89**: 243-253, DOI: 10.2151/jmsj.2011-305.

(Edited by Xie Jun)